

# Modular Structures for Manned Space Exploration: The Truncated Octahedron as a Building Block

O. L. de Weck\* , W. D. Nadir† , J. G. Wong‡ , G. Bounova§ and T. M. Coffee¶

*Massachusetts Institute of Technology, Cambridge, MA, 02139, USA*

Modular space exploration systems have been built in the past and they exist today. Most of these systems, starting with Apollo and Soyuz, assign high level functions to various physical spacecraft modules and assemble these in a linear stack. The predominant building block for such systems is the cylinder. Unfortunately, this configuration is inflexible and does not promote reuse of modules over a broad range of missions. We argue that future space exploration systems should be reconfigurable and therefore require additional docking ports, reconfiguration options and improved structural and volumetric efficiency. A survey of the modular spacecraft literature and our own analysis reveal that the truncated octahedron emerges as the most promising polyhedron-based spacecraft geometry for future application to space exploration. This argument is supported by comparison of various spacecraft geometries with four metrics: volumetric efficiency, launch stowage and packing efficiency, reconfigurability, and stability. In addition, extensible spacecraft design is enabled by this design concept. This is shown in a preliminary design of manned exploration vehicles based on the truncated octahedron concept in which a mass penalty in designing a modular version of a Mars transfer and surface habitat vehicle compared to a “point design,” linear stack concept, was found to be approximately 25%.

## Nomenclature

$a$	Edge length of octahedron
$A$	Surface area, $m^2$
$b$	Edge length of truncated octahedron
$D_{cs}$	Truncated octahedron circumsphere diameter, $m$
$D_{hex}$	Truncated octahedron hexagonal face insphere diameter, $m$
$D_{mod}$	Module diameter, $m$
$D_{sq}$	Truncated octahedron square face insphere diameter, $m$
$f_{ECLS}$	Environmental control and life support system recovery factor
$f_{fill}$	Propellant tank fill fraction
$f_{mod}$	Structural modularity mass scaling penalty factor
$f_{propscale}$	Propulsion system scaling factor
$f_{oxfill}$	Oxidizer tank fill fraction
$i$	Total number of non-redundant design configurations
$J$	Objective function
$m$	Mass, $kg$
$n$	Number of modules

\*Assistant Professor, deweck@mit.edu, Department of Aeronautics and Astronautics and Engineering Systems Division, Room 33-410, 77 Massachusetts Ave., Cambridge, MA, USA, AIAA Senior Member.

†Graduate Research Assistant, bnadir@mit.edu, Department of Aeronautics and Astronautics, Room 33-409, 77 Massachusetts Ave., Cambridge, MA, USA, AIAA Student Member.

‡Undergraduate Researcher, wongj@mit.edu, Department of Aeronautics and Astronautics, 77 Massachusetts Ave., Cambridge, MA, AIAA Student Member.

§Graduate Research Assistant, gergana@mit.edu, Department of Aeronautics and Astronautics, Room 37-346, 77 Massachusetts Ave., Cambridge, MA, USA, AIAA Student Member.

¶Undergraduate Researcher, tcoffee@mit.edu, Department of Aeronautics and Astronautics, 77 Massachusetts Ave., Cambridge, MA, USA, AIAA Student Member.

$N_{crew}$	Number of crew
$N_{LV}$	Total number of launches required
$N_{mod}$	Number of modules
$s$	Substitutability
$\Delta t_{man}$	Manned duration, days
$u$	Number of new-to-firm modules
$V$	Volume, $m^3$
$\delta$	Degree of coupling
$\mu_j$	Design reconfigurability for a structural system of $j$ design elements

## I. Introduction

THE traditional paradigm in modular, manned spacecraft design has been to create a linearly stacked sequence of modules, which are either launched together on a single, heavy-lift launch vehicle or launched separately on smaller launchers with subsequent assembly in Low Earth Orbit (LEO). Typically each of the modules is assigned a different high level function, and the modules carry out their function in one or more of the primary mission phases. Figure 1 shows an example of an extensible space transportation system based on this linear stacking paradigm.<sup>1</sup> This is similar to the Apollo/Soyuz design philosophy, but adds the aspect of extensibility of the modular stack for more and more ambitious missions. For missions to and from the International Space Station (ISS), one can envision a command module (CM) for housing crew, life support systems, attitude control systems as well as communications gear and other electronics. The nose of the CM is equipped with a docking port for human access. The service module (SM) provides consumables for the crew, stores propellant and contains the main engine(s). This stack can be extended by an orbital (maneuvering) module (OM) for extended operations in Low Earth Orbit. For more challenging missions with higher  $\Delta V$ s an extended service module (ESM) could be substituted. Finally, one may want the ability to add a transfer module (TM) for planetary transfer operations to the moon or to Mars. As Figure 1 shows, each module is based on a cylindrical structure, each featuring two manned, or unmanned docking interfaces front and aft. While this scheme is simple, it has two major drawbacks:

1. The number of possible configurations of a linear stack of  $N$  modules is small,  $N!$  at best, but is likely to be much smaller due to docking/interface restrictions.
2. The stack cannot be grown arbitrarily large, because the inertia matrix of the entire assembly becomes increasingly ill-conditioned with each additional module. Pencil-like structures are difficult to control in space (see Explorer I experience<sup>2</sup>).

In this paper we explore non-linear stacking sequences for modular, manned spacecraft. This requires considering alternate geometrical building blocks. After briefly reviewing the literature on modular spacecraft (Section II) we propose the truncated octahedron as an interesting alternative building block (Section III). After discussing the construction of this particular convex polyhedron, we show how multiple truncated octahedra can be connected to form various linear and non-linear stacks. Trying to quantify the number of possible configurations that can be assembled in this way leads to a brief excursion into mathematical tiling theory (Section A). In order to compare modular spacecraft building blocks we develop four metrics:

1. Volume/Surface ratio as a measure of volumetric efficiency (Section B)
2. Close-packing and launch stowage packing efficiencies (Section B)
3. Reconfigurability coefficient, i.e. number of possible configurations over number of modules,  $N$  (Section B)
4. Spacecraft stability (see Section VII)

Another way to frame this paper is by considering current modular space systems in two and three dimensions. Two-dimensional modules are increasingly attractive for antennas, solar arrays and optical mirrors (Figure 2 upper row). While sparse, circular apertures have been proposed it can safely be said that hexagonal panels are finding increasing use because of their close-packing properties (small or no gaps

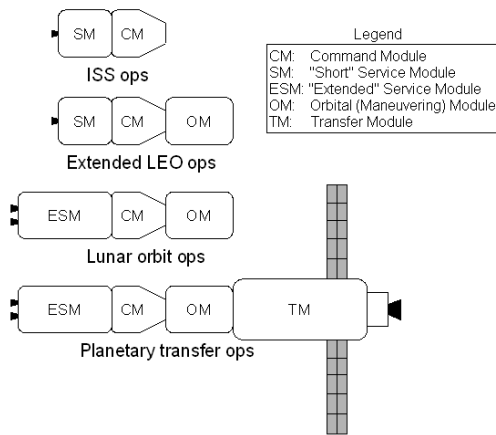


Figure 1. Linear stack, modular architecture.

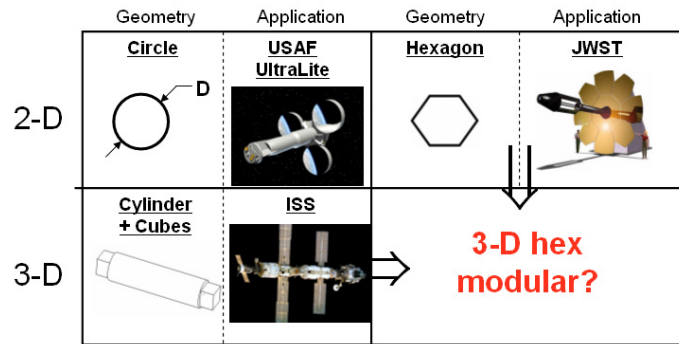


Figure 2. Extensibility of two and three-dimensional space structures.

when assembled side-by-side) as well as their advantageous surface area-to-circumference ratio. In three-dimensional space structures we have mainly relied on a combination of cylindrical elements, with cube-based connecting nodes (ISS), see Figure 2 lower left. One may wonder if there exists a hexagon-based three-dimensional geometry that may serve as building block for efficient manned (or unmanned) spacecraft modules.

## II. Literature Review

As early as 1985, engineers had begun to recognize the limitations of the cylinder as the shape of basic spacecraft modules. Frisina points out the need for close-packable modules that maintain modularity without creating the voids associated with cylinders when stacked together.<sup>3</sup> In 1994, Frisina proposed the isosceles tetrahedron as the basic unit from which to construct modules that do not create voids when stacked together. Triangular beams constitute the basic tetrahedral grid on which engineers can attach triangular faces, permitting reconfigurability.<sup>4</sup>

Though such a technique would be practical for construction of large enclosed spaces, such as a space hangar, it would be infeasible for the creation of modules. Certain essential subsystems, like avionics, propulsion and life support, must be connected in fixed topologies. Modularizing a spacecraft arbitrarily may break these critical connections.

Some space designers recognize the need to reduce the cost of design by introducing common components to families of space missions similar in design requirements. Five proposed platform designs, including two from the 1980's, extol the virtues of common hardware components and interfaces. These are proposed by Parkinson,<sup>5</sup> Mikulas and Dorsey,<sup>6</sup> Whelan, et. al.,<sup>7</sup> Miller,<sup>8</sup> and Smithies et al.,<sup>9</sup> with an emphasis on extensibility and cost reduction. Daniels and Saavedra of EER Systems<sup>10</sup> offer a modular platform for launch vehicles. The explosion of space platform literature following the appearance of modularity literature indicates cross-fertilization of ideas occurred.

In addition, the literature from the past two decades points to a realization of the need for standardized spacecraft interfaces. Baily, et al.,<sup>11</sup> Harwood and Ridenoure,<sup>12</sup> and Abbott of Ontario Engineering International<sup>13</sup> offer different proposals for standardized interfaces.

The movement toward modular thinking in spacecraft design is largely motivated by cost. At the end of the Cold War, cost, rather than performance, became the dominant priority in program budgets.<sup>14</sup> Changes in foreign policy could no longer justify the tremendous costs associated with space transport and space activity could continue only by adopting the "commercial attitude" of cost reduction.<sup>15</sup> The cost of on-orbit assembly, an enabling technology for modular spacecraft design, has been modeled by Morgenthaler.<sup>16</sup>

Modularity enables designers to reduce cost by amortizing, over many missions, the cost of developing and producing common components.<sup>17</sup> Additionally, modularity accelerates development by enabling different groups to work on different modules simultaneously. Modularity also lowers the cost of spacecraft diversification by confining development to only the modules that must be changed for different missions.

In general, the design flexibility of modularity enables firms to respond much more quickly to changes in budgets and market-driven goals.

However, modularity has a few disadvantages. In order to accommodate future innovation, modular designs require a larger upfront cost than do “integral” or “monolithic” designs.<sup>14</sup> In addition, modular designs create a mass penalty on missions that require less performance than the design offers, and create a performance penalty on missions that require more performance than the design offers.

While it is common for modular designs to be sub-optimal as a single vehicle, optimality over the entire lifecycle of a space system favors modular systems.

Quantification of modularity permits the consideration of modularity in analyses such as cost-benefit and design tradeoffs. Mikkola and Gassmann examined many other measures of modularity, and proposed a new non-dimensional measure of modularity as a function of the percentage  $u/N$  of modules that are new-to-firm (NTF), the degree of coupling,  $\delta$ , and substitutability,  $s$ .<sup>18</sup>

NTF modules are newly developed modules that combine with existing modules (termed “standard components” by Mikkola and Gassmann) to form new products. NTF modules incur development and qualification costs, but confer upon the firm proprietary advantage.  $u$  is the number of NTF modules.  $N$  is the total number of modules.

The degree of coupling measures the dependence of a module on its interactions with the rest of the system to function.  $d$  is the average of the ratios of total number of interfaces to number of components of each subsystem of the product.

Substitutability is the ease with which modules can be swapped in order to create new products or to increase product variety. The substitutability factor  $s$  “is estimated as the number of product families made possible by the average number of interfaces of NTF components [modules] required for functionality.”<sup>18</sup>

Because the rate of modularity decrease is dependent on the existing degree of modularity, the relation is exponential, as shown in Equation 1.

$$M = \exp \frac{-u^2}{2Ns\delta} \quad (1)$$

As the number of total modules increases, the modularity decreases less quickly. Thus, the more modules there are, the greater the modularity, behavior that is consonant with intuition. It is possible that all variables may not be used in all analyses. In analyses where all variables are not used, the unused variables can be controlled. Indeed, Mikkola and Gassmann present the modularization function only as a function of  $u$ .

The following section presents the truncated octahedron as a concept for modular, structural design.

### III. The Truncated Octahedron Concept

#### A. Properties and Construction of the Truncated Octahedron

The truncated octahedron is a fourteen-sided polyhedron composed of six square faces and eight hexagonal faces. All edges of the truncated octahedron have equal length. A truncated octahedron can be created by joining two square pyramids together at their bases to form an octahedron and then cutting all six corners to remove one-third of the edge length from each vertex. The resulting truncated octahedron has edges that are all one third the length of the “parent” octahedron. The relationship between the edge length of an octahedron and a truncated octahedron is shown in Equation 2.

$$b = \frac{a}{3} \quad (2)$$

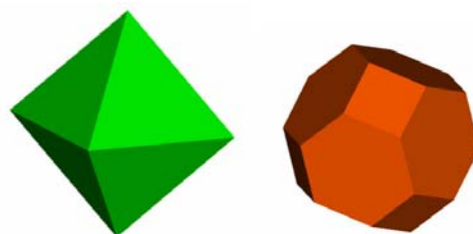


Figure 3. Left: equilateral octahedron with edge length  $a$ . Right: regular truncated octahedron with edge length  $b$ .

#### B. Truncated Octahedron Insphere

In order to estimate an internal usable volume of a truncated octahedron-shaped spacecraft, the equation defining a completely inscribed sphere in the truncated octahedron was determined. This “hex” insphere, tangent to the hexagonal faces of the polyhedron, is defined in Equation 3. Since there are both hexagonal and square faces in a truncated octahedron, there is also an

insphere related to the square faces. This inscribed sphere is not as useful, however, because parts of this sphere are external to the polyhedron. The equation defining the “square” insphere is Equation 4. These inspheres are shown in Figure 4.

$$D_{hex} = \sqrt{6}b \quad (3)$$

$$D_{sq} = 2\sqrt{2}b \quad (4)$$

In Equations 3 and 4,  $D_{hex}$  is the diameter of the “hex” insphere,  $D_{sq}$  is the diameter of the “square” insphere, and  $b$  is the edge length of the truncated octahedron.

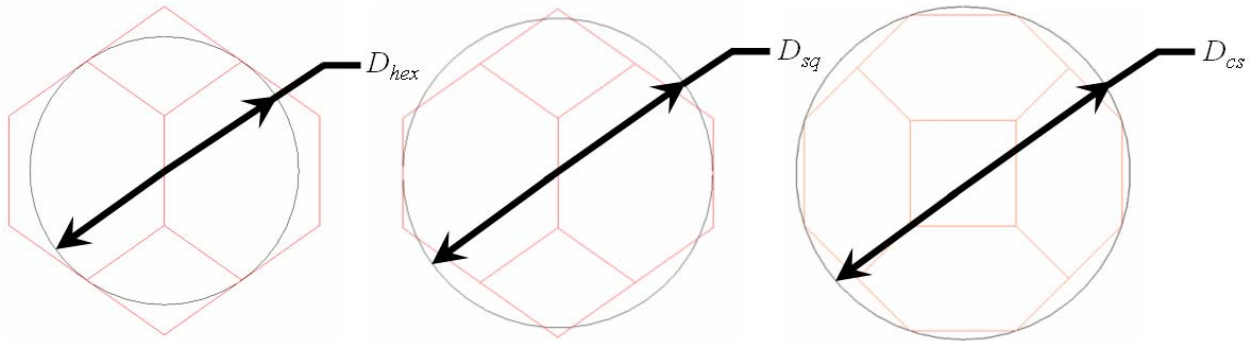


Figure 4. Hexagonal insphere (left), square insphere (center), and circumsphere (right) diameters.

### C. Truncated Octahedron Circumsphere

A useful dimension for determining the envelope of the truncated octahedron is the circumspherical diameter,  $D_{cs}$ . For example, this dimension is used to size modules which fit inside a specific launch fairing. The circumsphere is a sphere in which the truncated octahedron is inscribed (see Figure 4).

$$D_{cs} = \sqrt{10}b \quad (5)$$

### D. Analogs in Nature

Close approximations to hexagonal partitioning as well as truncated octahedron partitioning can be found in nature. Sandpipers in the tundra, terns on the barrier islands off North Carolina, and bottom-living African cichlid fish in a breeding tank all exhibit hexagonal partitioning.<sup>19</sup> The most famous case in nature of hexagonal partitioning are honeycombs and larval cells of bees and wasps, shown in Figure 5.<sup>20</sup> Close approximations of truncated octahedra can be made by compressing a container filled with lead shot until the shot deforms enough to squeeze out all the air in the container.<sup>19</sup> In addition, the thin-walled cells that fill the middles of the stems of many herbaceous plants approach the ideal truncated octahedron shape with about fourteen faces on each.<sup>19</sup>



Figure 5. Bee with honeycomb.

### E. Multi-Octahedron Configurations

The truncated octahedron allows for the creation of different structural design configurations. Three basic configurations possible with this modular building block are the linear stack, ring, and “sphere.” These concepts are shown in Figure 7. The ability of the truncated octahedron module to attach at a square face, hexagonal face, or a combination of faces results in a large, but finite number of unique configurations if more modules are added to the structural system.

The linear stack concept is useful for a small number of modules launched in a single launch vehicle since the payload fairing is a cylindrical shape. The ring design may be useful for a spinning transfer habitat to provide artificial gravity for the astronauts. The spherical structure concept is useful for improving spacecraft

stability, compacting structure for protection by a heat shield during atmospheric entry, and for radiation protection. Plume impingement during aerocapture or atmospheric entry can be reduced using this concept.

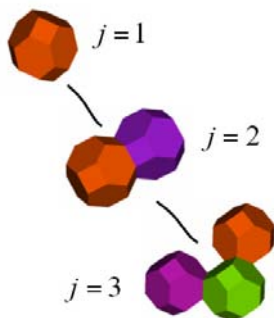


Figure 6. Modular structural designs with increasing numbers of design elements,  $j$ .

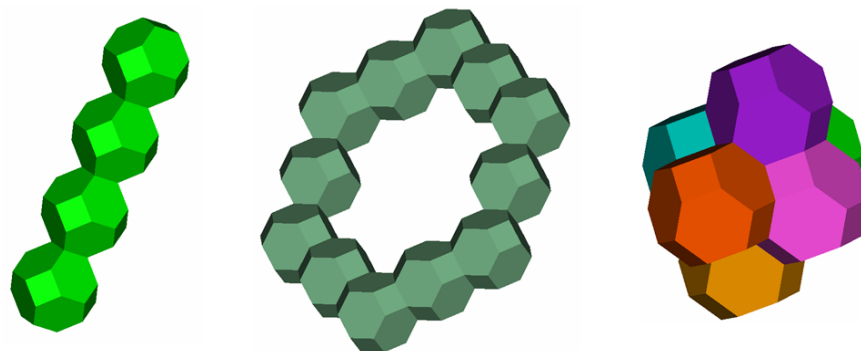


Figure 7. Linear stack, ring, and “sphere” truncated octahedron configuration concepts.

## IV. Comparison of Building Block Geometries

### A. Mathematical Tiling Theory

The notional utility of the truncated octahedron concept can be formalized via the theory of combinatorial tiling. We restrict ourselves here to close-packing polyhedra, that is, solid shapes capable of completely filling three-dimensional space. This limits the scope of candidate geometries, but appears advantageous for storage, reconfigurability, and structural robustness.

We define a three-dimensional tiling as a system of polyhedra (called tiles) that covers three-dimensional Euclidean space and for which the intersection of any two tiles is either an empty set, common vertex, common edge, or common face. A three-dimensional tiling is called periodic if there exists a *crystallographic space group*—a discrete group of isometries on three-dimensional Euclidean space containing three linearly independent translations—that maps the points and faces of the tiling onto itself.

Two tilings are topologically equivalent if there is a homeomorphism mapping the tiles of one onto the tiles of the other. They are called homeomeric if their space groups are also equivalent under the homeomorphism. Note that in each topological equivalence class there will be a tiling exhibiting maximum symmetry; the other members of the class may be derived from it by so-called “symmetry breaking,” creating additional degrees of freedom in the tiling structure.

Finally, we call two tiles equivalent if there is a symmetry in the space group of the tiling that maps one tile to the other. We define equivalence similarly for vertices, edges, and faces. When these constituents have a finite number  $k$  of equivalence classes, we call the tiling *vertex-*, *edge-*, *face-*, or *tile- $k$ -transitive* as appropriate.

For candidate geometries, we will restrict ourselves to *face- $k$ -transitive* tilings: this will allow modular interfaces to be effectively utilized. A surprising result in combinatorial tiling theory<sup>21</sup> shows that the number of *face- $k$ -transitive* tilings is finite: in fact, there exist only 88 such tilings, falling into seven topological equivalence classes. These classes are defined by the following symmetries: tetrahedron, cube, octahedron, rhombic dodecahedron, special rhombohedron, and covered rhombohedron.

Strong candidates for modular spacecraft geometry may be derived from the maximally symmetric elements of these classes: less symmetric elements are likely to exhibit poorer surface area-to-volume ratios and weaker reconfigurability with no gains in packing efficiency. Though general proofs have yet to be constructed, empirical analysis of the metrics in Section B shows the truncated octahedron to be among the most favorable among these possibilities.

## B. Metrics: Volumetric and Launch Efficiencies and Reconfigurability

For analysis in space systems we will develop a set of, perhaps simpler, metrics which measure a set of desirable properties of individual spacecraft modules and their combinations:

1. **Reconfigurability Coefficient:** Design reconfigurability is defined as the number of non-redundant design configurations,  $i$ , divided by the total number of design elements,  $j$ .
2. **Volume/Surface Area:**  $V/A$ , this ratio is a measure of the volumetric efficiency of a module. One of the goals of space system design is to maximize the amount of usable volume (e.g. for crew habitation, equipment installation or storage of consumables), while minimizing the mass needed to contain the volume. This metric applies to a single module.
3. **Packing Efficiency:** This is the ratio of filled volume over the total enveloping volume of a set of modules that are closely packed. We distinguish between close-packing efficiency (deployed on orbit) and launch stowage efficiency (inside a launch vehicle fairing).

## C. Design Reconfigurability

For the purposes of this study, design reconfigurability of a modular spacecraft structural design is defined as the number of non-redundant design configurations divided by the total number of unique design elements used. The equation defining this metric,  $\mu$ , is shown in Equation 6. In the equation,  $i$  is the total number of possible non-redundant design configurations given a number of design elements,  $j$ . In this case, design elements are considered to be identically-sized truncated octahedron modules.

$$\mu_j = \frac{i}{j}, \text{ where } j = 1, 2, \dots, \infty \quad (6)$$

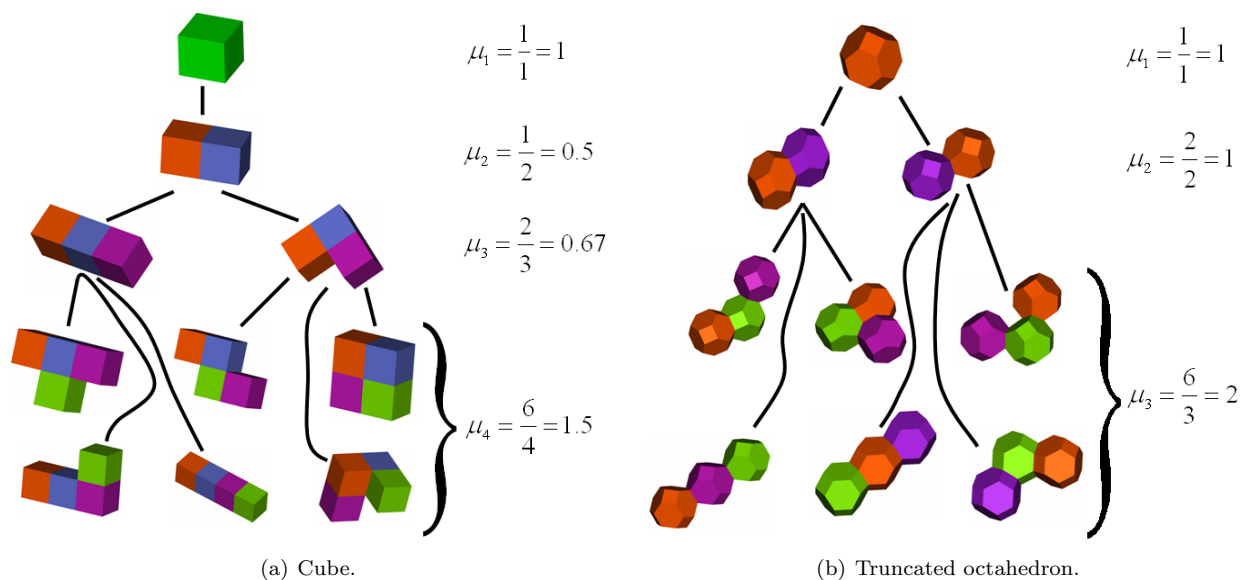


Figure 8. Design reconfigurability trees for the cube and truncated octahedron.

It is assumed that each face of the truncated octahedron can mate with an identical face of another truncated octahedron. The two mating faces must be oriented such that the edges are aligned. As more design elements are added, the complexity of the design increases significantly. Non-redundant configurations are unique designs which are created by using  $j$  design elements. Both square and hexagonal faces are considered for docking. In addition, configurations are restricted to those which preserve the close-packing property of the truncated octahedron. This restricts the angle at which each module is oriented with respect to the corresponding mate. An illustration of how the number of unique configurations depends on the number of design elements is shown in Figure 8 for the truncated octahedron and cube. All faces of the cube are assumed to be able to mate with all faces of other cubes because all faces are of equal dimensions.

The design reconfigurability of the truncated octahedron and the cube are compared in Figure 9. The truncated octahedron exhibits a greater design reconfigurability than the cube as more elements are added to the structural design configuration. The dashed line is included in the figure for the truncated octahedron design reconfigurability for greater than three design elements because this performance for the truncated octahedron has yet to be computed. However, the trends shown in the figure are indicative of the design flexibility performance of the truncated octahedron for greater numbers of design elements. It is likely the truncated octahedron will continue to outperform the cube for even greater numbers of design elements.

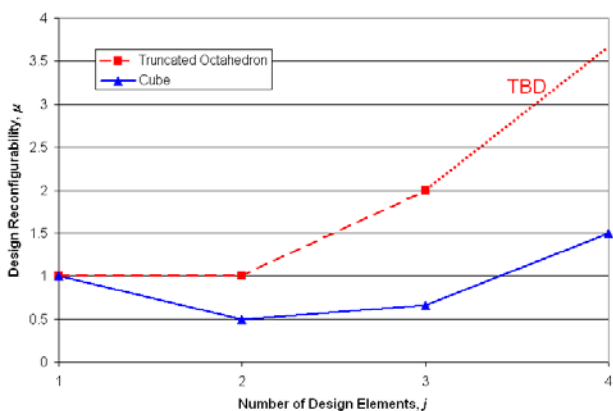


Figure 9. Design reconfigurability comparison of the truncated octahedron and cube.

#### D. Volume-to-Surface Area Ratio

For a pressurized volume spacecraft structure, the volume-to-surface area ratio is an important factor to consider. Ideally, a spherical structure would be used for a pressurized volume since it would result in evenly-distributed loading throughout the pressurized surface of the structure.

In reality, many pressurized volumes sent into space are not spherically-shaped. Fuel tanks generally are spherically-shaped, but crewed vehicles are usually cylindrical, cone-shaped, or have a custom shape. This is the case because of the interface requirements of these space structures. Fuel tanks do not require interfaces beyond simple structural mounting and pipes to transport fuel, oxidizer, and pressurant. Crewed pressurized structures, on the other hand, require large, flat interfaces for people and cargo to pass through. This large, flat interface requirement makes a spherical design for crewed space vehicles less practical. Cylindrical structures with interfaces on each end are usually the design of choice. The ISS is composed of many cylindrical, pressurized volume structures, for example. The truncated octahedron, in fact, has faces that can accommodate these interface requirements while maintaining a more favorable volume-to-surface area ratio.

The volume-to-surface area ratio of the truncated octahedron is compared to that of a sphere, cube, and cylinder. The results of this comparison are shown in Figure 10. It is assumed that each three-dimensional shape contains a unit volume. The truncated octahedron has the highest volume-to-surface area ratio of the non-spherical shapes considered. This is because the truncated octahedron more closely resembles a sphere than the other non spherical modules. The truncated octahedron's volume-to-surface area ratio performance is 91% as good as the sphere, 4% better than the cylinder at its most favorable aspect ratio, and 13% better than the cube.

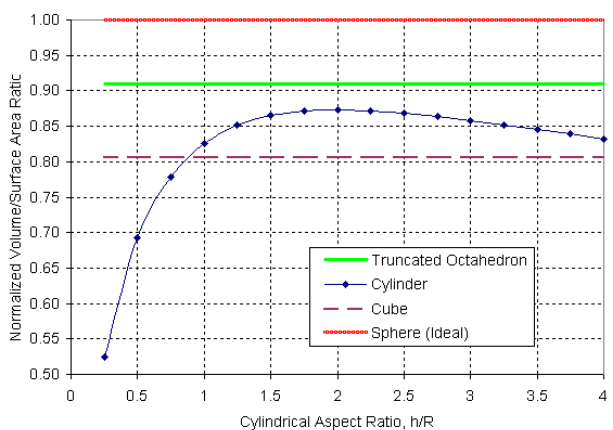


Figure 10. Volume-to-surface area ratio comparison of the sphere, truncated octahedron, cylinder, and cube.

#### E. Packing Efficiency

The packing efficiency of a structural modular building block is important for the stowed and deployed configurations of a space structure. The stowed configuration is defined as the structure as configured in the launch vehicle fairing. The deployed configuration is the final, assembled structure in space.

The ability of the truncated octahedron to pack together without voids results in perfect deployed packing efficiency. However, the stowed packing efficiency is somewhat inefficient due to the inability of large truncated octahedron modules to pack densely inside a cylindrical payload fairing. Whereas the cylinder may achieve close to 100% stowed packing efficiency compared to almost 50% for the truncated octahedron (see Table 1). However, whether or not launch stowage efficiency is acceptable depends on whether the mass limit or the volume limit is the active constraint. For *LOX* modules expect the former, for *LH<sub>2</sub>* modules expect the latter.

An important constraint which prevents better stowed efficiency results is the requirement that the circumspherical diameter,  $D_{cs}$ , be the value of the maximum usable launch fairing. This allows for the use of modules of such size for crewed missions. The smaller the module size, the more efficiently the fairing volume can be filled, but such small module sizes would not be useful for manned spacecraft. Examples of stowed packing configurations for the truncated octahedron are shown in Figure 11. The deployed packing efficiency of the truncated octahedron is 100% compared to 100% for the cube, 91% for the cylinder, and 78% for the sphere.

Launch Fairing	$D_{cs}$	No. of Modules	Stowed Efficiency
Delta IV, 4-m	3.75	2	46%
Delta IV, 5-m, sht.	4.57	2	48%
Delta IV, 5-m, lng.	4.57	3	48%
Atlas V, 5-m, sht.	4.57	1	27%
Atlas V, 5-m, med.	4.57	2	42%

**Table 1. Truncated octahedron stowed packing efficiency results.**

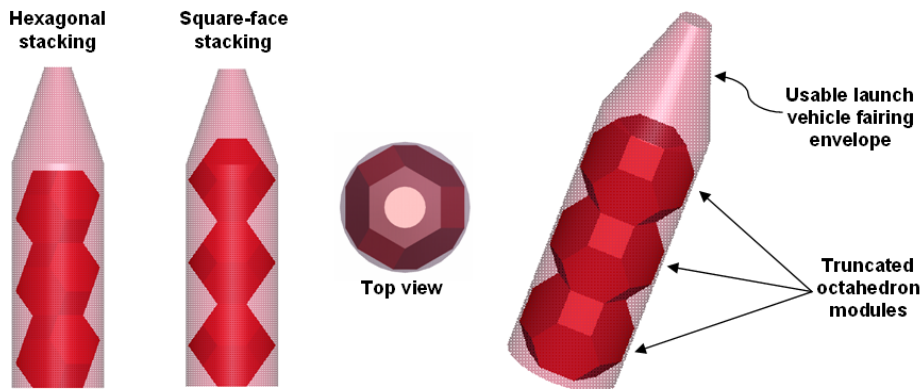


**Figure 11. Stowed packing visualizations of truncated octahedron for the Delta IV, 5-meter, long fairing.**

## V. Structural Design Application: NASA CER Vehicle Modularization

The space exploration initiative set forth by the current US administration calls for the manned exploration of the Moon, Mars, and beyond. The initiative requires an affordable exploration system design to ensure program sustainability.<sup>22</sup> This section presents a methodology for incorporating modularity into spacecraft structural design to help achieve sustainable, affordable space exploration. In addition, the modularization presented in this section is used to demonstrate the use of the truncated octahedron as a structural building block for space applications.

### A. Transportation Architectures

Mars and Moon mission architectures developed by the MIT Fall 2004 16.981 Advanced Special Projects class working on the NASA Concept Evaluation and Refinement study for President Bush's space exploration initiative are used for motivation for this design example.<sup>23,24</sup> The vehicle to be modularized to investigate the benefits of the truncated octahedron is the Transfer and Surface Habitat (TSH) defined in a Mars mission architecture (see Figure 12).<sup>23-25</sup>

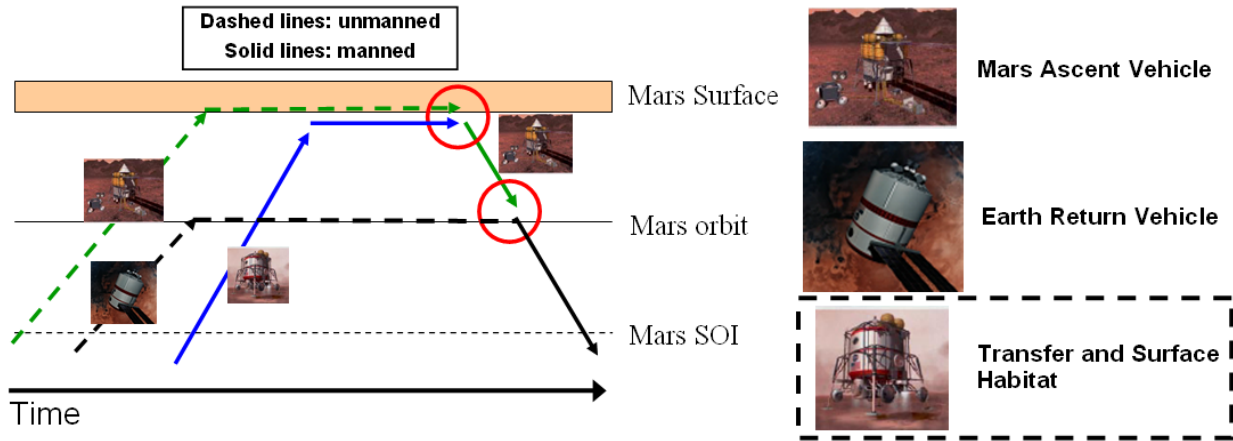


Figure 12. Example Mars mission architecture.

### B. “Point Design” Analysis

The Mars architecture selected for this analysis is similar to NASA’s Mars Design Reference Mission.<sup>25</sup> This architecture includes three vehicles: the Mars Ascent Vehicle (MAV), Earth Return Vehicle (ERV), and TSH. The MAV and ERV are prepositioned at Mars and it is verified that they are functioning properly before the crew travels to Mars. The crew of six travels to Mars in the TSH, lands, lives for 500 days on the surface, enters the MAV, launches into LMO, transfers to the ERV, travels back to Earth, and lands on Earth in the Earth Entry Module. It is assumed that each vehicle uses aerocapture at Mars instead of a propulsive orbit insertion. Mission architecture trajectory information is shown in Table 2.<sup>23</sup> TMI and TEI stand for trans-Mars injection and trans-Earth injection, respectively.

Traj.	Fuel/Oxidizer Used	$\Delta V$ (m/s)	Trans. Time (days)
TMI	$LH_2/LOX$	3600	260
TEI	$LCH_4/LOX$	2115	260

Table 2. Mars mission architecture trajectory details.

Component	MAV (mT)	ERV (mT)	TSH (mT)
Earth Entry Module	-	12.0	-
Habitat	3.6	52.9	<b>62.1</b>
TEI stage dry	-	8.0	-
TEI stage prop	-	53.1	-
Mars ascent stage dry	1.4	-	-
Mars ascent stage prop	9.0	-	-
Mars descent stage dry	1.4	-	<b>6.3</b>
Mars descent stage prop	2.7	-	<b>12.1</b>
Heat shield	3.6	25.2	<b>16.1</b>
TMI stage dry	5.1	35.2	<b>22.5</b>
TMI stage prop	33.8	234.9	<b>150.0</b>
Total mass	60.7	421.3	<b>269.0</b>

Table 3. Mars mission architecture vehicle mass breakdowns.

Based on calculations performed by the MIT 16.981 class,<sup>23,24</sup> detailed mass breakdowns for the vehicles used in this architecture were calculated. These masses are included in Table 3.<sup>23</sup>

### 1. Design Constraints

The design constraints considered for modularization of the Transfer and Surface Habitat are imposed by the launch vehicle. For this analysis, an upgraded Delta IV Heavy launch vehicle is assumed to be the only launch vehicle system used. Based on information from Boeing about upgradability of the Delta IV,<sup>26</sup> a Delta IV with a 6.5 meter diameter fairing and a payload capability of 40,000 kg to LEO is assumed. The assumed upgraded Delta IV Heavy launch fairing dimensions can be seen in Figure 13.<sup>26, 27</sup>

### 2. Assumptions

In order to compare the modular version of the TSH, a non-modular version must be designed. This “point design” of the TSH is assumed to be composed of cylindrical, linearly-stacked components. These components are the following: the descent module (DM), the transfer and surface habitat module, and the TMI orbit transfer module. The cylindrical dimensions of the habitat and propulsion modules are limited by the launch vehicle constraints as defined in Section 1.

### 3. Transfer and Surface Habitat Module Design

The high-level design of the habitat in the TSH was performed by estimating the mass and volume. The pressurized volume required for this module is determined from the number of crew and the manned duration of the habitat. The pressurized volume required per crew member is assumed to be  $19 \text{ m}^3$ .<sup>28</sup> The manned duration of this habitat is approximately 760 days.

Once the volume required per crew member,  $V_{habitable}$ , is known, the total pressurized volume,  $V_{pressurized}$ , is calculated using Equation 7. The number of crew,  $N_{crew}$ , is six for this mission. The pressurized volume required for this habitat is  $342 \text{ m}^3$ .

$$V_{pressurized} = 3V_{habitable}N_{crew} \quad (7)$$

The total mass of the habitat is determined using Equation 8, an equation based on historical data for human spacecraft modules which has been modified for mission durations greater than 200 days.<sup>23, 29</sup>

$$m_{hab} = 592 (N_{crew} \Delta t_{man} V_{pressurized})^{0.346} + N_{crew} f_{ECLS} \dot{m}_{cons} (\Delta t_{man} - 200) \quad (8)$$

In Equation 8,  $\Delta t_{man}$  is the duration the habitat is crewed in days,  $f_{ECLS}$  is the environmental control and life support system (ECLS) recovery factor, set to a value of 0.68,<sup>30</sup> and  $\dot{m}_{cons}$  is the mass flow rate of consumption of consumables per crew member in kilograms per day, set to a value of 9.5 based on Apollo mission data.<sup>30</sup> The resulting habitat mass is determined to be 62,070 kg.

### 4. Orbit Transfer Module Design

The Orbit Transfer Module (OTM), a large, single-stage propulsion module used to provide the  $\Delta V$  for the TMI leg of the Mars mission, consists of large propellant tanks and an engine. Given the payload being transported to Mars, the rocket equation, shown in Equation 9, is used to size the OTM. The specific impulse,  $I_{sp}$ , and mass ratio of the  $LOX/LH_2$  propellant are 450 seconds and 6:1, respectively.<sup>31</sup> The payload for the OTM,  $m_{pl}$ , consists of Mars landing stage, habitat, and aerocapture heat shield with a combined mass of 96,564 kg. The propulsion system mass fractions used for propellant tanks and engines are 0.113 and 0.037, respectively.<sup>23</sup> The detailed initial and final mass breakdowns are shown in Equations 10 and 11, respectively. The OTM propulsion system masses were calculated using the equations

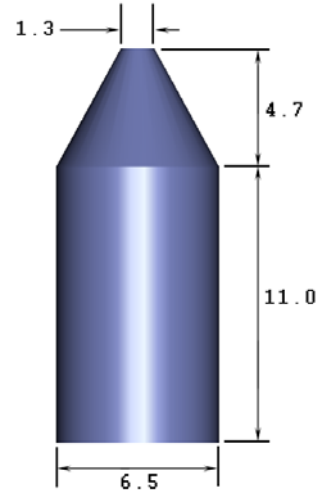


Figure 13. Upgraded Delta IV Heavy launch vehicle fairing (dimensions in meters).

Prop	Mass (kg)	Density ( $kg/m^3$ )	Vol. ( $m^3$ )
$LH_2$	21,430	70.8	302.7
$LOX$	128,570	1141	112.7

Table 4. OTM propellant mass breakdown.

mentioned previously. Propellant masses are shown in Table 4. In addition, a dry mass of 22,500 kg is determined using a dry mass fraction of 15%.

$$\Delta V = I_{sp}g_0 \ln \left( \frac{m_0}{m_f} \right) \quad (9)$$

$$m_0 = m_{pl} + m_{prop} + m_{tank} + m_{eng} \quad (10)$$

$$m_f = m_{pl} + m_{tank} + m_{eng} \quad (11)$$

In Equations 9, 10, and 11,  $m_0$  is initial mass,  $m_f$  is final mass,  $m_{prop}$  is propellant mass,  $m_{tank}$  is propellant tank mass, and  $m_{eng}$  is engine mass.

### 5. Heat Shield Mass Estimation

The mass of the heat shield,  $m_{hs}$ , required for aerocapture of the habitat and descent module of the TSH is estimated using Equation 12. The factor of 20% used in this equation is selected to roughly approximate the mass of the heat shield. While this factor does not produce an accurate heat shield mass, it adequately represents the heat shield for the purposes of this analysis.

$$m_{hs} = 0.2 (\text{protected mass}) \quad (12)$$

### 6. Design Solution

Using the masses and volumes for the “point design” TSH vehicle, shown in Figure 14, a CAD model is created with the calculated volumes and mass properties of the landing stage, habitat, OTM, and heat shield. Solar cell arrays are included in the CAD model for illustrative purposes but are not used for mass properties analysis.

## C. Vehicle Modularization

In order to incorporate modularity using the truncated octahedron concept for TSH design, three parts of the vehicle are selected for modularization: the habitat, fuel tank, and oxidizer tank. Truncated octahedron-shaped modules are used to create the required structures for each of the selected components.

### 1. Modularization Assumptions

A set of assumptions is used to perform the modularization of the Transfer and Surface Habitat vehicle. First, the hexagonal insphere (see Section B for definition) is used to determine the estimated internal pressurized volume of a truncated octahedron module. Second, the circumsphere diameter of the module is the benchmark for determining the size of the module. This sphere is useful for determining the envelope of the module for stowage in a launch vehicle fairing. Third, a structural modularity factor,  $f_{mod}$ , of 10% is assumed. This modularity factor is included to account for the overall structural mass increase from the additional structure required to enclose smaller volumes than the one-module “point design.” Finally, a docking hardware penalty,  $m_{dock}$ , of 400 kg per module is assumed. This mass penalty accounts for standardized docking hardware between modules and extra hardware required for the facilitation of electronic, thermal, environmental, and propellant transport between modules.

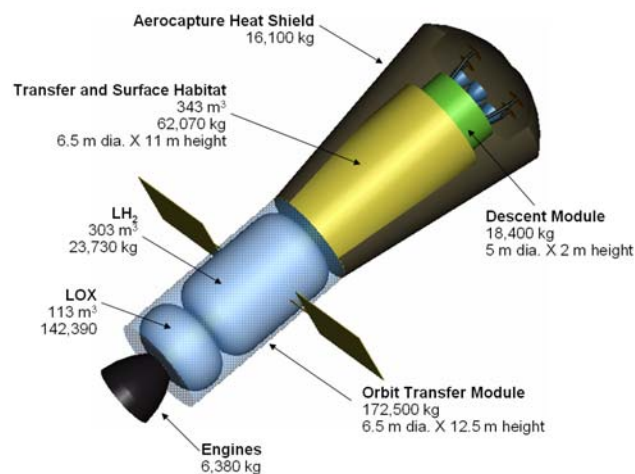


Figure 14. Linear stack “point design” vehicle (heat shield partially removed for habitat and descent module viewing).

## 2. Design Objectives

Two design objectives,  $J_1$  and  $J_2$ , are used to determine the “optimal” modular quanta for vehicle components.  $J_1$  and  $J_2$  are the number of launches required to put the complete vehicle in LEO,  $N_{launches}$ , and the total initial mass in LEO (IMLEO),  $m_{IMLEO}$ , respectively. These objectives are both functions of three variables, the truncated octahedron module circumsphere diameter,  $D_{mod}$ , a propulsion system scaling factor,  $f_{propscale}$ , and an oxidizer tank fill factor,  $f_{oxfill}$ . These objective functions are shown in Equations 13 and 14.

$$J_1(D_{mod}, f_{propscale}, f_{oxfill}) = N_{launches} \quad (13)$$

$$J_2(D_{mod}, f_{propscale}, f_{oxfill}) = m_{IMLEO} \quad (14)$$

## 3. Design Variables

Three design variables are used to search the modular quanta design space. These design variables are a propulsion system scaling factor,  $f_{propscale}$ , an oxidizer tank fill factor,  $f_{oxfill}$ , and the truncated octahedron circumsphere module diameter,  $D_{mod}$ . The propulsion system scaling factor is a design variable because it needs to be adjusted in order for the  $\Delta V$  constraint to be satisfied depending on the modular quanta selected. The oxidizer tank fill factor is used to allow for the feasibility of large propulsion tank sizes while still satisfying the launch vehicle payload mass constraint by only partially filling the oxidizer tanks. This allows for the possibility of investigating larger modular sizes even though liquid oxygen, a very dense liquid, is one of the propellants.  $D_{mod}$  is used to determine the “optimal” truncated octahedron module size to select for the modular spacecraft design.

## 4. Design Constraints

The primary constraints for the modularization of the TSH vehicle are the launch vehicle constraints detailed in Section 1 and the  $\Delta V$  requirement of 3,600 m/s for the TMI burn in the Mars architecture (see Table 2). In addition, all modules used for the spacecraft design must have the same circumsphere diameter. This allows habitat, fuel tank, and oxidizer tank modules to all fit together properly to take advantage of the packing efficiency and manufacturing cost benefits of the truncated octahedron modular design. The upper bound for the module diameter is the launch vehicle fairing diameter. The lower bound of 4.4 meters for the module diameter is selected to be a reasonable number based on the internal dimensions necessary for useful manned spacecraft design. These constraints are shown in Equations 15, 16, 17, 18, 19, and 20.

$$\Delta V_{sys} \geq 3600 m/s \quad (15)$$

$$m_{habmod}, m_{oxmod}, m_{fuelmod} \leq 40,000 kg \quad (16)$$

$$D_{mod} = D_{habmod} = D_{oxmod} = D_{fuelmod} \quad (17)$$

$$4.4m \leq D_{mod} \leq 6.5m \quad (18)$$

$$0 \leq f_{propscale} \leq 1 \quad (19)$$

$$0 < f_{oxfill} \leq 1 \quad (20)$$

In the design constraint equations,  $\Delta V_{sys}$  is the velocity change imparted on the spacecraft for the TMI mission segment. The mass of each habitat, oxidizer tank, and fuel tank module is denoted by  $m_{habmod}$ ,  $m_{oxmod}$ , and  $m_{fuelmod}$ , respectively. The circumsphere diameter of each habitat, oxidizer tank, and fuel tank module is denoted by  $D_{habmod}$ ,  $D_{oxmod}$ , and  $D_{fuelmod}$ , respectively. The modular quanta diameter is denoted by  $D_{mod}$ .

## 5. Module Sizing Procedure

A flow chart of the procedure used to create modular designs is shown in Figure 15. First, the masses and volumes of the components of the system to be modularized are specified (see Figure 14 for these values). Second, the propellant volume to be used is scaled by the  $f_{prop\,scale}$  design variable to allow for  $\Delta V$  feasibility. This scaling factor allows for a more simplified set of calculations by eliminating the need to iterate propulsion system wet and dry masses to “optimally” size the modules while satisfying the  $\Delta V$  constraint. Third, the components to be modularized are subdivided into design interpolation points (see following Section). Fourth, the fill fraction of the oxidizer tanks is specified which determines the number of oxidizer tanks required. Fifth, the constrained design space is explored for the range of module sizes considered. The total IMLEO and number of launches of each feasible design is calculated and all feasible results are output and recorded for analysis.

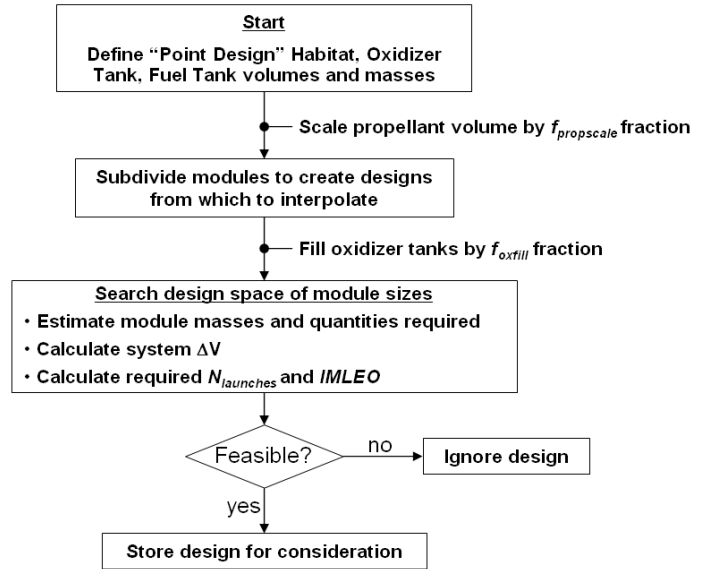


Figure 15. Modular sizing process flow chart.

## 6. Subdivision of Modules

To obtain masses of modules of various sizes, module design interpolation points are required. This is done by subdividing the original “point design ” volumes into smaller pieces, providing design reference points for which the module sizes being investigated use as interpolation reference points for the mass calculations of each habitat, fuel tank, and oxidizer tank module. An example of the modularization of the habitat component is shown in Table 5.

$N_{mod}$	$D_{mod}$ (m)	$V_{I_{mod}}$ ( $m^3$ )	$M_{I_{mod}}$ (kg)
1	11.21	342	62,070
2	8.9	172	32,211
3	7.77	114	21,607
4	7.06	86	16,305
5	6.56	69	13,124
6	6.17	57	11,004
⋮	⋮	⋮	⋮

Table 5. Subdivision of the habitat portion of Trans-fer and Surface Habitat vehicle.

	Habitat	Oxidizer	Fuel
$N_{mod}$	12	5	14
$m_{I_{mod}}$ (kg)	5,718	36,589	2,554
$m_{I_{str}}$ (kg)	15,518	18,163	3,027
$V_{mod}$ ( $m^3$ )	28.6	28.6	28.6
$V_{I_{mod}}$ ( $m^3$ )	28.6	28.3	27.1
$m_{mod}$ (kg)	68,616	183,169	35,930

Table 6. Example of calculation of tank module masses for  $D_{mod}$  of 4.9 meters,  $f_{prop\,scale}$  of 0.25, and  $f_{ox\,fill}$  of 1.0.

In order to calculate the mass of a 6.2 meter diameter habitat module, for example, the design is sized-up from the closest interpolation design that is smaller than or equal to the design being investigated in size (6.17 meters). The volume ratio of the design being considered versus the interpolation point is used to size the structural mass of the 6.2 meter habitat module. Equation 21 is used to calculate the mass of the mass of the interpolation point module design  $m_{I_{mod}}$  and Equation 22 is used to estimate the total mass of the vehicle component being investigated,  $m_{mod}$  (e.g. habitat, oxidizer, fuel).

$$m_{I_{mod}} = \left( \frac{m_{lin}}{N_{mod}} \right) + f_{mod} \left( \frac{m_{linstr}}{N_{mod}} \right) + m_{dock} \quad (21)$$

$$m_{mod} = N_{mod} \left[ m_{I_{mod}} + \frac{m_{I_{str}}}{N_{mod}} \left( \frac{V_{mod}}{V_{I_{mod}}} - 1 \right) \right] \quad (22)$$

In Equation 21,  $m_{lin}$  is the total mass of the linear design component being modularized and  $m_{linstr}$  is the dry mass of the component.

In Equation 22,  $m_{mod}$  is the total mass of a set of modules being investigated (i.e. habitat, oxidizer, fuel),  $N_{mod}$  is the number of modules required for the component,  $m_{I_{str}}$  is the structural mass of the interpolation point module design,  $V_{mod}$  is the volume of the module being investigated, and  $V_{I_{mod}}$  is the volume of the interpolation point module design. An example of how  $m_{mod}$  is calculated for a given module diameter is shown in Table 6.

### 7. Calculation of Required Number of Launches

The number of upgraded Delta IV Heavy launches required to put the entire TSH vehicle in LEO is calculated using the mass, size, and quantity of modules required. A set of rules is used to determine the launch manifests. First, only modules of the same type are launched together. Second, modules are packed “in-line” in the fairing. Third, a 14.25 meter limit for module stacking height in launch vehicle fairing is imposed (see Figure 16). This height limit is the maximum height a quantity of three 4.75 meter diameter modules can be stacked within the fairing envelope. A maximum quantity of two modules of diameter from 4.75 to 6.5 meters can be stored in the fairing as well.

Using the launch vehicle fairing constraints described above, the launch vehicle payload constraint, and the quantities and masses of modules to be launched, the total number of launches required can be calculated. Equations 23, 24, 25, and 26 are used to perform this calculation.

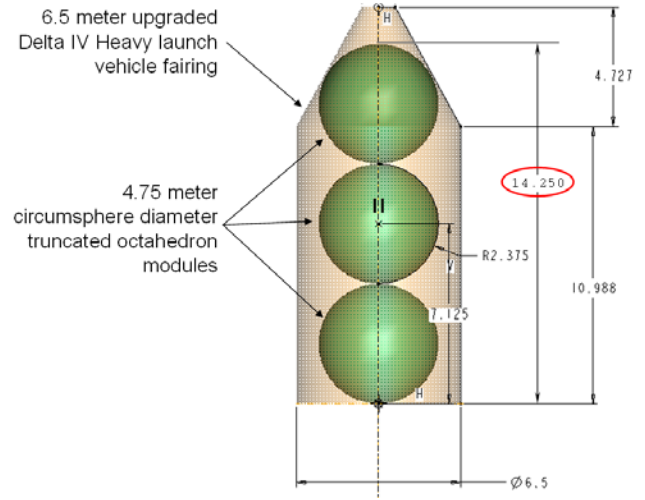


**Figure 16. Upgraded Delta IV Heavy fairing loaded with truncated octahedron modules. 14.25 meter module stacking height limit shown.<sup>26,27</sup> All dimensions are in meters.**

$$N_{LVdim} = \left\lfloor \frac{H_{limit}}{D_{mod}} \right\rfloor \quad (23)$$

$$N_{LVmass} = \left\lfloor \frac{m_{limit}}{m_{mod}} \right\rfloor \quad (24)$$

$$N_{LVmod} = \min(N_{LVdim}, N_{LVmass}) \quad (25)$$

$$N_{LV} = \sum_{i=1}^3 \left\lfloor \frac{N_{mod}}{N_{LVmod}} \right\rfloor_i \quad (26)$$

In the equations used to calculate the number of required launches,  $N_{LVdim}$  is the number of modules the launch vehicle can transport to LEO based only on dimension constraints,  $N_{LVmass}$  is the number of modules the launch vehicle can transport to LEO based only on mass constraints,  $H_{limit}$  is the launch fairing height limit,  $m_{limit}$  is the mass limit of the launch vehicle,  $m_{mod}$  is the mass of a module,  $N_{LVmod}$  is the number of modules the launch vehicle can transport to LEO, and  $N_{LV}$  is the total number of launches required for the vehicle. In Equation 26, the range of  $i$  is 1 to 3 because there are three types of modules considered in this modularization analysis.

### 8. Modularization Results

After searching the modularization design space using a spreadsheet, objective function results are obtained. These results are shown in Figure 17. The non dominated designs are connected by the dashed line to denote a possible Pareto front. In general,  $f_{oxfill}$  is increasing for designs as the total IMLEO mass decreases. Also,  $f_{propscale}$  increases as IMLEO mass and number of launches increase.

The “optimal” modular design selected based on the objective space search is the truncated octahedron with a circumsphere diameter of 4.9 meters with the propellant volume increased by 25% and the oxidizer tanks filled to capacity. This design was selected because it nearly has the minimal number of launches required and the design has the minimum IMLEO mass.

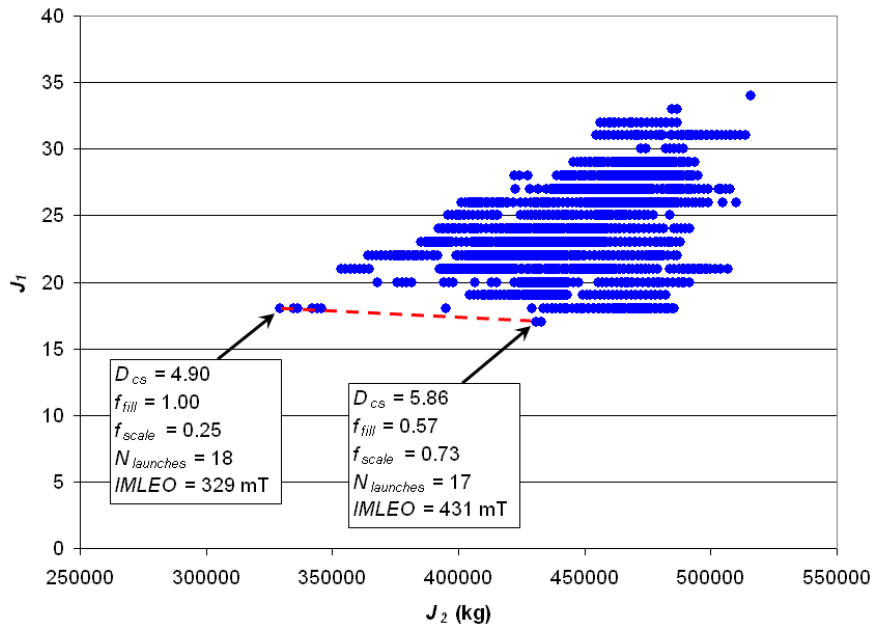


Figure 17. Modularization objective space results with non-dominated designs labeled.

The “optimal” modular design is composed of twelve habitat modules, five oxidizer tanks, and fourteen fuel tanks. The interpolation point designs used are shown in Figure 18. In this figure, the interpolation points used for this design are labeled and the corresponding number of modules is shown.

An additional feasibility check was performed to ensure the “optimal” modular vehicle design will have the  $\Delta V$  necessary to successfully perform the Mars exploration mission. The results for this check are shown in Figure 19. A large range of module sizes are infeasible due to their violation of the launch vehicle payload mass constraint. The maximum size was constrained to be the size at which the heaviest module is at the payload mass limit.

### 9. Modular Design Solution

The resulting modular design solution is shown in Figure 20. Using a  $D_{cs}$  value of 4.9 from the analysis performed in the previous sections, a spacecraft was designed with identically-sized habitat, fuel tanks, and oxidizer tanks. In Table 7, the modular and linear design masses are compared.

From the exploded spacecraft view in Figure 20, the interconnectivity between spacecraft modules can be visualized. The habitat is formed into a pyramid-like structure and the oxidizer tanks are assembled into a shape that fits into the center of a ring-like structure of fuel modules. The engines are assembled to the spacecraft to both fuel and oxidizer tanks at each of the four locations. The Mars descent propulsion stage is stacked on top of the habitat and a heat shield is used to protect the descent stage and habitat for aerocapture at Mars. Detailed structural interconnections between modules, the descent propulsion stage, and the heat shield are beyond the scope of this analysis and therefore have been omitted from the design presented.

### 10. Sensitivity Analysis

Sensitivity analysis was performed for modularization mass penalty design parameters. These design parameters are the docking hardware penalty,  $m_{dock}$ , and the structural modularity penalty,  $f_{mod}$  (see Section 1). The sensitivity of each objective with respect to two design parameters is investigated. The Jacobian

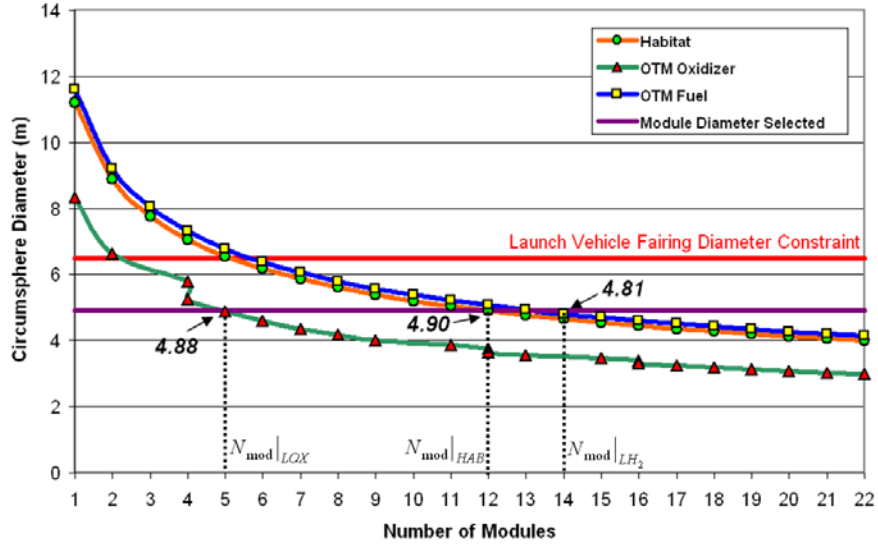


Figure 18. Modularization design interpolation points with “optimal” design interpolation points and constraints shown.

Component	$N_{mod}$	$m_{mod}$ (kg)	Module Mass, $\frac{m_{mod}}{N_{mod}}$ (kg)	Linear Design Mass (kg)	Modular Design Volume ( $m^3$ )	Point Design Volume ( $m^3$ )
Habitat	12	68,422	5702	62,100	343	343
$LO_X$ prop.	5	162,000	32,400	128,570	143	113
$LH_2$ prop.	14	31,500	2,250	21,430	401	303
$LO_X$ dry	5	22,000	4,400	18,160	N/A	N/A
$LH_2$ dry	14	8,820	630	3,030	N/A	N/A
Heat shield	1	16,094	16,094	16,100	N/A	N/A
Lander	1	18,400	18,400	18,400	N/A	N/A
Engines	4	7,720	1,930	5,550	N/A	N/A

Table 7. Comparison of modular and optimal Transfer and Surface Habitat vehicle component masses.

matrix, shown in Equation 27, is determined for the two objective, two parameter sensitivity analysis. For the calculation of the partial derivatives, various step sizes were investigated to determine if the derivative is dependent on the step size. Step sizes of 25, 50, and 100 kilograms for  $m_{dock}$  and 0.0125, 0.025, and 0.05 for  $f_{mod}$  are investigated. Based on this investigation, it is determined that the derivatives are not dependent on step size.

$$\nabla J(\mathbf{x}^0) = \begin{bmatrix} \frac{\partial J_1}{\partial m_{dock}} & \frac{\partial J_2}{\partial m_{dock}} \\ \frac{\partial J_1}{\partial f_{mod}} & \frac{\partial J_2}{\partial f_{mod}} \end{bmatrix}_{\mathbf{x}^0} = \begin{bmatrix} 31 & 0 \\ 36708 & 0 \end{bmatrix} \quad (27)$$

In Equation 27,  $\mathbf{x}^0$  is the “optimal” design vector used for this analysis.

To obtain more useful sensitivity results, the terms in the Jacobian are normalized. The normalization factors used are an approximate method to normalize the Jacobian terms. The origin of the normalization factor is shown in Equation 28 with more detail in Equation 29.

$$\frac{\Delta J/J}{\Delta p_i/p_i} \simeq \frac{p_{i,0}}{J(\mathbf{x}^0)} \cdot \nabla J(\mathbf{x}^0) \quad (28)$$

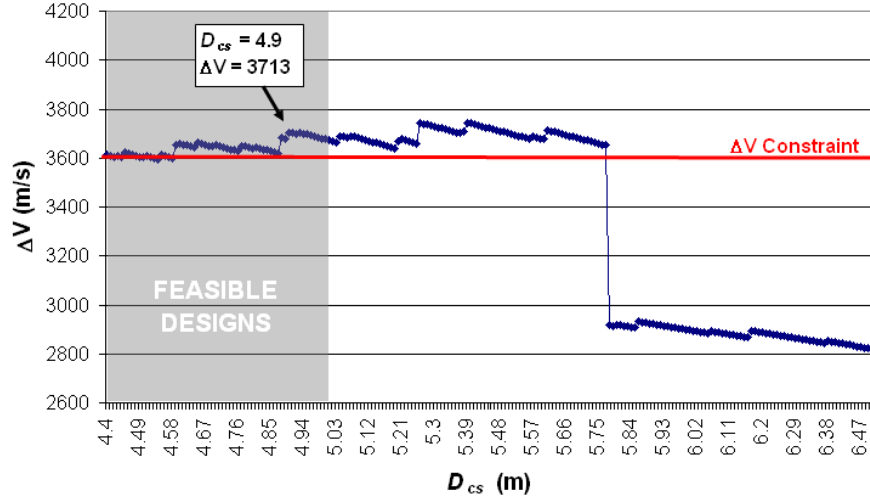


Figure 19. Modular spacecraft  $\Delta V$  results for module sizes with “optimal” modular design variable settings.

$$p_{i,0} = \left[ \begin{array}{cc} \frac{\partial m_{dock}(\mathbf{x}^0)}{\partial J_1(\mathbf{x}^0)} & \frac{\partial m_{dock}(\mathbf{x}^0)}{\partial J_2(\mathbf{x}^0)} \\ \frac{\partial f_{mod}(\mathbf{x}^0)}{\partial J_1(\mathbf{x}^0)} & \frac{\partial f_{mod}(\mathbf{x}^0)}{\partial J_2(\mathbf{x}^0)} \end{array} \right] \quad (29)$$

In Equation 28,  $p_{i,0}$  is the  $i^{th}$  design parameter (for  $i = 1, 2$ ) at the “optimal” design point,  $\mathbf{x}^0$ . From this equation, the normalized sensitivities of the two objectives with respect to each design parameter are determined. These results are shown in Table 8.

The sensitivity analysis results show the  $J_1$  objective, total IMLEO, is sensitive to both design parameters with  $J_1$  being roughly three times more sensitive to a change in  $m_{dock}$  than to  $f_{mod}$ . The practical meaning of these normalized sensitivity values is that a 100% increase in the value of  $m_{dock}$ , for example, will result in an increase in  $J_1$  of 3.8%, or approximately 12,500 kg. The  $J_2$  design objective, number of launches required, is not sensitive at all to either of the design parameters. The relatively small effect of the parameter settings on the design objectives reduces the importance of how closely these parameter settings match to realistic mass penalties associated with modularization.

Design Parameter	$J_1$ Norm. Sensitivity	$J_2$ Norm. Sensitivity
$m_{dock}$	0.038	0.000
$f_{mod}$	0.011	0.000

Table 8. Sensitivity analysis results for modularization mass penalty design parameters.

## VI. Lunar Variant Analysis and Design

In this section, a transfer and surface habitat vehicle is designed for a Moon mission based on the Mars mission architecture in Section A. This lunar transfer and surface habitat is built using components of the TSH used for the Mars mission. This design approach is called “Mars back.”

### A. “Mars Back” Design

A major benefit of modular spacecraft design is the ability to design extensibility into a space exploration system. Extensible design can improve the affordability for a system to explore the Moon and Mars, ultimately enhancing the sustainability of the program. Extensibility is incorporated into such an exploration system using a “Mars-back” vehicle design approach. A “Mars-back” approach means the exploration system hardware is designed for Mars missions with the ability of the same or similar hardware to be used in advance during Moon missions. This has the effect of eliminating the cost of developing a suite of Moon-specific hardware as well as Mars-specific hardware and instead develop one set of dual use hardware. In addition, since this hardware design is composed of identical building block structures, the cost of integration, assembly, and testing of the hardware will be reduced due to learning curve cost savings and the ability to streamline

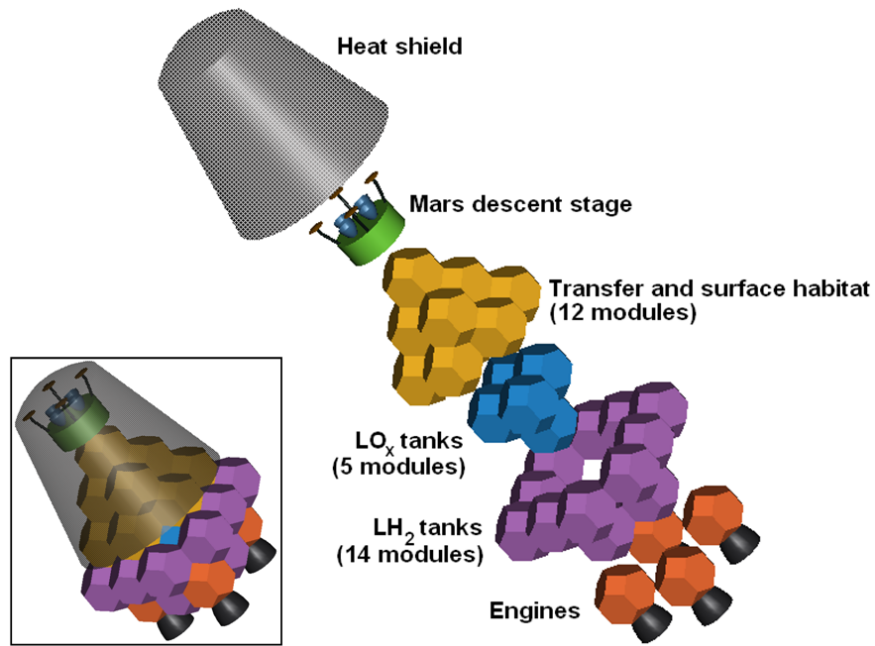


Figure 20. Exploded and unexploded views of modular TSH vehicle design (heat shield translucent for viewing of hidden components). Solar panels not included in figure.

and automate the process.

## B. Lunar Variant Architecture

In this section, hardware from the transfer and surface habitat vehicle designed in Section V will be used to create a vehicle for a Moon mission. The Moon mission used is called a “lunar variant” since the vehicles used are variants of those used for Mars missions. The lunar variant architecture selected for this analysis, similar to work done by the MIT Fall 2004 16.981 Advanced Special Projects class, is shown in Figure 21.<sup>23–25</sup> The vehicle selected for “Mars-back” design is the transfer and surface habitat (TSH) vehicle, with similar functionality to the TSH vehicle used in the Mars architecture. Relevant lunar variant TSH vehicle information for this architecture is shown in Table 9.<sup>32,33</sup>

Mission Phase	$\Delta V(m/s)$	Duration (days)
TMI	3,150	3.5
LOI	850	0.5
Descent	2,083	0.5
Surface ops	N/A	180
Total	6,083	184.5

Table 9.  $\Delta V$  and duration information for lunar variant architecture.

## C. Analysis Assumptions

Several assumptions have been made to perform this analysis. First, the total  $\Delta V$  needed to be performed by the TSH propulsion system is assumed to be the sum of the  $\Delta V$ s needed for all three burns (see Table 9). Second, the propellants selected for the engine are the same as in the Mars mission spacecraft design example. Third, the fuel and oxidizer tanks are allowed to be partially filled with propellant. In addition, a crew of four is assumed to be flying on this lunar exploration mission as opposed to a crew size of six for the Mars mission described earlier in this chapter. Finally, a volume of  $19m^3$  is assumed again for each crew member for the lunar variant TSH vehicle.

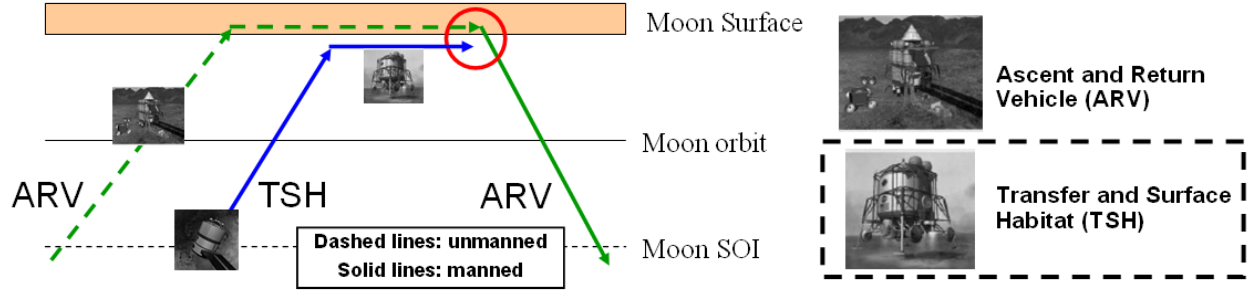


Figure 21. Example lunar variant architecture.

#### D. Habitat Mass Estimation

The first step to estimate the total lunar variant TSH habitat mass,  $m_{habLV}$ , is to determine the dry mass of each habitat module,  $m_{hab_{mod}}^{dry}$ . This mass is determined using the Mars mission TSH habitat design according to the “Mars back” design approach. This mass estimate was obtained by subtracting the total consumables required for the Mars TSH habitat,  $m_{hab}^{cons}$ , from the total TSH habitat mass,  $m_{hab}$ . The remaining mass is then divided by the total number of Mars TSH habitat modules,  $N_{mod_{hab}}$ , to obtain the result. This is shown in Equations 30 and 31. In addition, Equation 30 is used with lunar mission parameters to determine the total consumables required for the lunar mission habitat,  $m_{habLV}^{cons}$ .

$$m_{cons_{hab}} = N_{crew} f_{ECLS} \dot{m}_{cons} (\Delta t_{man}) \quad (30)$$

$$m_{hab_{mod}}^{dry} = \frac{m_{hab} - m_{hab}^{cons}}{N_{mod_{hab}}} \quad (31)$$

In Equation 30, a variant of Equation 8 is used and again the required consumables mass flow rate,  $\dot{m}_{cons}$ , is assumed to be  $9.5 \text{ kg/crew/day}$ .<sup>23,30</sup>

Next, the required habitat volume for the lunar variant habitat,  $V_{habLV}$ , is determined using Equation 7 for lunar mission parameters. The number of lunar mission habitat modules,  $N_{mod_{habLV}}$ , is determined using Equation 32 by comparing  $V_{habLV}$  to the Mars mission required habitat volume,  $V_{hab}$ . Due to the volume-per-crew constraint, the crew size drives habitat volume rather than the mission duration.

Finally, Equation 33 is used to determine the total lunar variant habitat mass. Results for this analysis are shown in Table 10.

$$N_{mod_{habLV}} = \left\lceil N_{mod_{hab}} \left( \frac{V_{habLV}}{V_{hab}} \right) \right\rceil \quad (32)$$

$$m_{habLV} = m_{habLV}^{cons} + N_{mod_{habLV}} m_{hab_{mod}}^{dry} \quad (33)$$

Parameter	Description	Mars Mission	Lunar Variant
$V_{hab}$	Total habitat volume ( $m^3$ )	343	228
$N_{mod_{hab}}$	No. habitat modules	12	8
$m_{hab_{mod}}^{dry}$	Dry mass per module ( $kg$ )	3,239	3,239
$m_{hab}^{cons}/N_{mod_{hab}}$	Consumables mass per module ( $kg$ )	2,463	596
$m_{mod_{hab}}$	Total mass per module ( $kg$ )	5,702	3,835
$m_{hab}$	Total habitat mass ( $kg$ )	68,422	30,679

Table 10. Mass calculation results for lunar variant habitat.

## E. Propulsion System Sizing

For the lunar variant TSH mission, oxidizer and fuel tanks sized according to the Mars TSH mission are used. The propulsion system is sized in order to satisfy the  $\Delta V$  requirement of 6,083  $m/s$ . The rocket equation (see Equation 9) is used to perform this analysis. Maintaining the required oxidizer/fuel mass ratio, the mass of oxidizer is used as a variable to size the overall propulsion system to search for feasible designs. The number of fuel and oxidizer tanks is determined such that there are enough to contain all fuel and oxidizer required. Equations 34, 35, and 36 are used to perform this analysis.

$$N_{mod_{LOX}} = \left\lceil \frac{V_{LOX}}{V_{mod}} \right\rceil \quad (34)$$

$$N_{mod_{LH_2}} = \left\lceil \frac{V_{LH_2}}{V_{mod}} \right\rceil \quad (35)$$

$$\Delta V = g_0 I_{sp} \ln \left( \frac{m_{habLV} + N_{mod_{LOX}} m_{LOX}^{dry} + N_{mod_{LH_2}} m_{LH_2}^{dry} + m_{LOX}^{prop} + m_{LH_2}^{prop}}{m_{habLV} + N_{mod_{LOX}} m_{LOX}^{dry} + N_{mod_{LH_2}} m_{LH_2}^{dry}} \right) \quad (36)$$

$N_{mod_{LOX}}$  and  $N_{mod_{LH_2}}$  are the number of oxidizer and fuel modules required, respectively.  $V_{LOX}$  and  $V_{LH_2}$  are the total required volumes of oxidizer and fuel, respectively.  $m_{LOX}^{dry}$  and  $m_{LH_2}^{dry}$  are the dry masses of each oxidizer and fuel module, respectively (see Table 7 for reference).  $m_{LOX}^{prop}$  and  $m_{LH_2}^{prop}$  are the total propellant masses of oxidizer and fuel, respectively.

Figure 22 shows how scaling the size of the propulsion system affects  $\Delta V$  performance. This data was used to select the best lunar variant design by choosing the lowest IMLEO configuration. The curve is not linear due to dry mass increases of additional propellant modules required for additional propellant volume. Detailed mass results for the selected configuration are shown in Table 11.

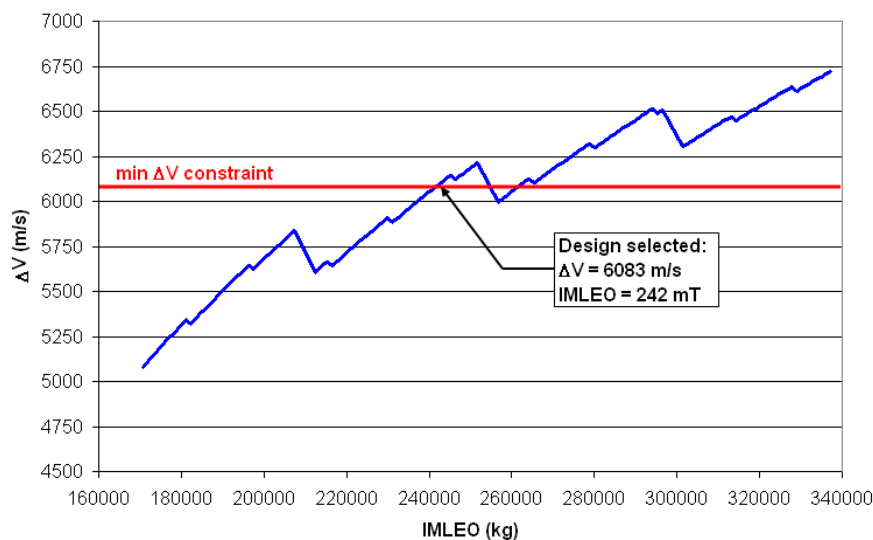


Figure 22. Lunar variant TSH vehicle propulsion system scaling  $\Delta V$  versus IMLEO performance.

Parameter	Description	Oxidizer, $LOX$	Fuel, $LH_2$
$N_{mod}$	Number of modules ( $m^3$ )	5	13
$N_{mod} \cdot m^{dry}$	Total dry mass ( $kg$ )	22,000	8,190
$m^{prop}$	Total propellant mass ( $kg$ )	155,500	25,900
$f_{fill}$	Tank fill percentage (%)	95	98

Table 11. Mass calculation results for lunar variant propulsion system.

## F. “Mars back” Design Conclusions

A vehicle used for a Moon exploration mission is created using elements designed for a mission to Mars. The modular design of the TSH vehicle allows for this design extensibility. Significant cost savings potential can result from leveraging spacecraft designs from one set of missions to another in this manner. Although the design extensibility of one vehicle is shown in this example, this process should be feasible for other vehicles in the architectures presented. In fact, extensibility may be possible between different vehicles for the same mission, an analysis which may be performed in future work. A side-by-side visualization of the TSH vehicles designed for Mars and Moon missions is shown in Figure 23.

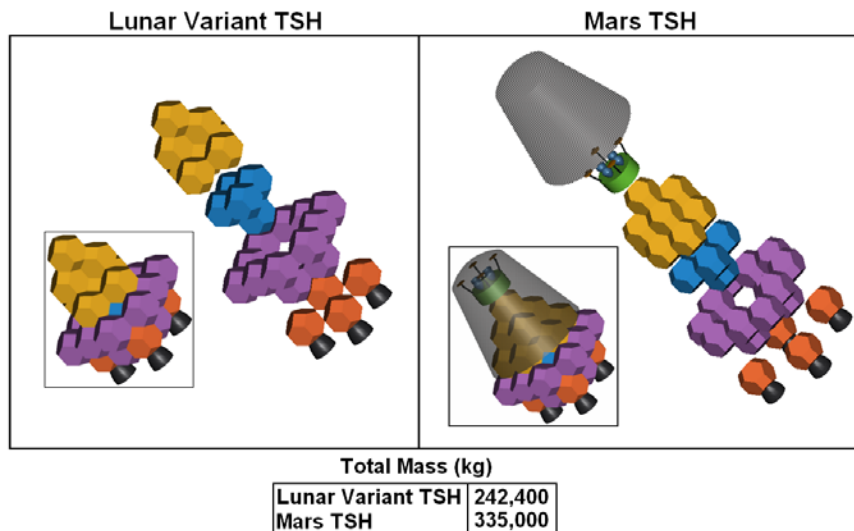


Figure 23. Extensible TSH vehicle combinations: Mars and lunar variant TSH configurations.

## VII. Modular Vehicle Stability Benefits

This section highlights several stability benefits of modular spacecraft design. These benefits are improved pitch stability, improved landing stability, and reduced thrust inaccuracy due to misalignment of the thruster and center of gravity.

### A. Pitch Stability

First, assume the linear and modular spacecraft are spin stabilized about the axes shown in Figure 25. In order to be stable in pitch, the spin axis of the spacecraft must be the axis of maximum moment of inertia (MOI).<sup>2</sup> While neither the linear or modular Mars exploration spacecraft designs from Section V are spin stabilized about their axis of maximum MOI (Y-axis), the relative difference in magnitude between the maximum MOI and the other moments of inertia for each spacecraft differs significantly. The MOI directions are shown in Figure 25 and the resulting principal moments of inertia of each spacecraft are shown in Table 12.

From Table 12, it is shown that the maximum principal moment of inertia axis for each spacecraft is in the Y-direction. However, the relative magnitude difference between the maximum principal moment of inertia and the other principal moments of inertia is significantly smaller for the modular spacecraft than the linear stack design. This means that while both spacecraft are unstable in pitch, the modular spacecraft is not as unstable as the linear stack design. In fact, a modular spacecraft could be assembled in a “pancake”

Moment of Inertia	Linear Design ( $kg \cdot m^2$ )	Modular Design ( $kg \cdot m^2$ )
$I_x$	$1.63 \times 10^7$	$8.28 \times 10^6$
$I_y$	$1.63 \times 10^7$	$8.72 \times 10^6$
$I_z$	$1.61 \times 10^6$	$4.23 \times 10^6$

Table 12. Mass calculation results for lunar variant propulsion system.

shape in which it would indeed be able to be spin stabilized about the maximum principal moment of inertial. This is infeasible with linear stack design concept due to the payload dimension limitations of the launch vehicle fairing.

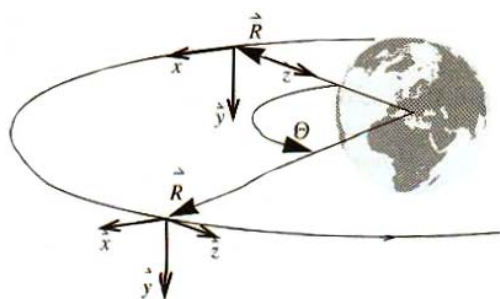


Figure 24. Body-fixed coordinate system and inertial flight attitude.

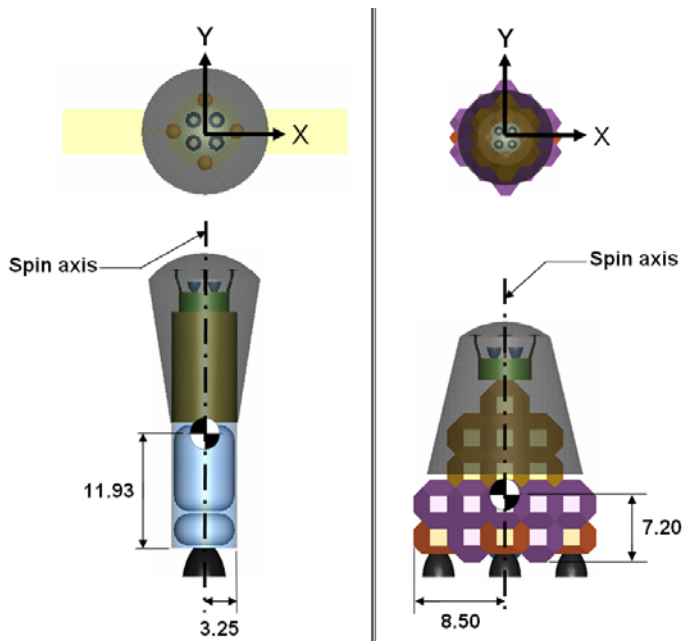


Figure 25. Linear and modular Mars TSH configurations with coordinate systems, spin axes, and moment arms labeled.

For vehicles in inertial flight mode, as assumed in this analysis, the radius vector in the body-fixed coordinate system can be described as follows in Equation 37. A revolution angle  $\Theta$ , corresponding to true anomaly, is introduced to describe the changing radius vector throughout an orbit. See Figure 24<sup>30</sup> for the coordinate system description of inertial flight mode.

$$\hat{R} = \begin{bmatrix} \sin \Theta \\ 0 \\ -\cos \Theta \end{bmatrix} \quad (37)$$

Assuming each spacecraft is in an inertial flight mode while in a circular orbit in LEO, the stability performance of each vehicle can be visualized as shown in Figure 27.<sup>34</sup> Based on the results in Figure 27, with respect to gravity gradient disturbance torques, both the linear and modular spacecraft are stable in yaw and roll but are unstable in pitch. The modular design is favorable because it more closely approximates a spherical-shaped spacecraft (located at the origin).

## B. Landing Stability

An important factor in the landing stability of a spacecraft is the height of the spacecraft center of gravity from the bottom of the landing structure. The smaller this dimension, the less “top heavy” the lander. The reduction in this dimension has the benefit of improving the stability of the lander by reducing the likelihood of the spacecraft toppling over during or after landing. A rough landing or high winds may cause the center of gravity of the lander to shift such that it may not be between the landing legs, causing

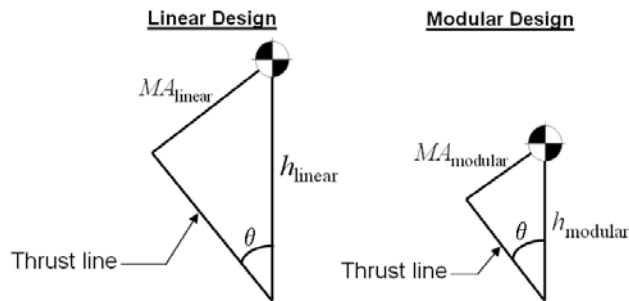


Figure 26. Thrust line distance from center of gravity for linear and modular spacecraft designs resulting from thrust misalignment angle,  $\Theta$ .

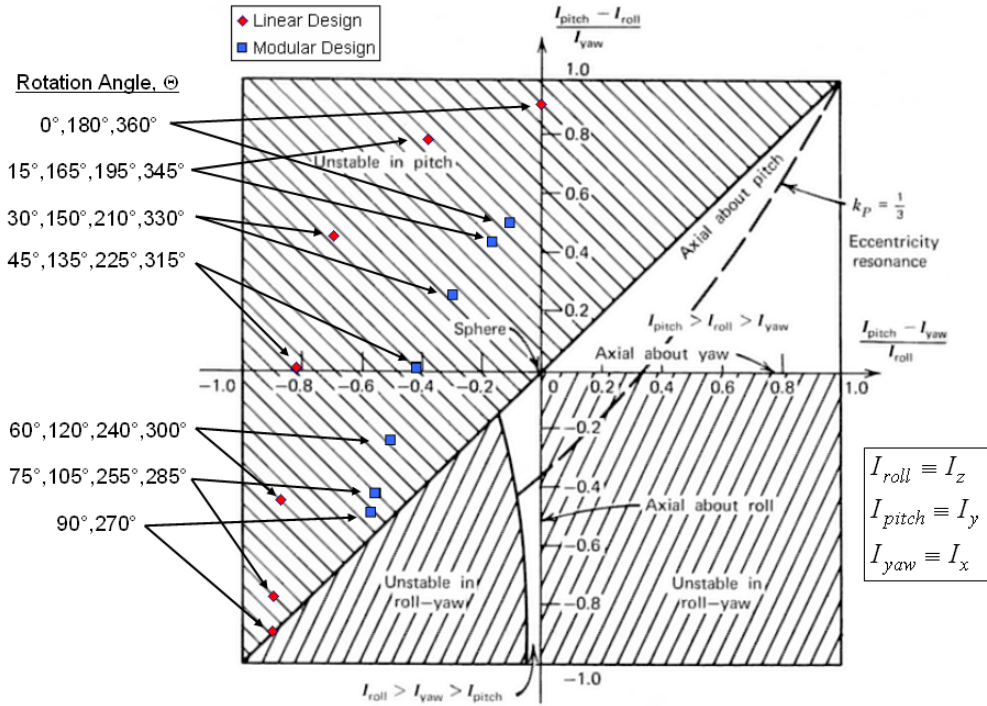


Figure 27. Gravity gradient stability regions with linear and modular spacecraft stability performance overlaid.

the spacecraft to topple over. However, a lower center of gravity will reduce the chances of encountering this toppling condition. As seen in Figure 25, the modular spacecraft has a smaller center of gravity height (7.20 meters) than the linear design (11.93 meters). The modular spacecraft design concept allows a wide array of configuration options for reducing this height as opposed to the long, cylindrical configuration of the linear stack concept.

### C. Thruster Misalignment

A third benefit to the configuration options provided by the modular spacecraft design concept is the ability to reduce the penalty associated with a thrust line misalignment with the center of gravity. If the thruster is misaligned, the thrust line does not pass directly through the center of gravity of the spacecraft. The burn error resulting from this misalignment requires that corrective propulsive maneuvers are performed to keep the spacecraft on the desired trajectory. The ability to reduce the distance between the thrust wall and spacecraft center of gravity modular design concept using the truncated octahedron (shown in Figure 25) helps reduce the distance of the center of gravity and the thrust line, helping reduce the burn error associated with thrust line misalignment. The geometrical benefit is shown in Figure 26.

In Figure 26,  $MA_{linear}$  and  $MA_{modular}$  are the distances between the thrust lines and centers of gravity for the linear and modular vehicle designs, respectively. Also,  $h_{linear}$  and  $h_{modular}$  are the distances between the centers of gravity and the thrust walls of the linear and modular vehicle designs, respectively. From Figure 26, it is clear that  $MA_{modular}$  is less than  $MA_{linear}$ . The resulting torque on the spacecraft from the misalignment is also reduced accordingly.

## VIII. Conclusion

The truncated octahedron is an efficient, modular geometry for potential use in human space exploration systems. This convex polyhedron approaches the volumetric efficiency of the sphere, but has no voids when closely packed (ideally). In fact, the truncated octahedron is claimed to be the three-dimensional solid that has the largest volume/surface-area ratio, while still being close-packing. The number of reconfigurations

allowed, on the other hand significantly exceeds those of the cylinder and the cube. The launch stowage efficiency is somewhat reduced compared to cylindrical structures, but it is unclear whether this is a real disadvantage in cases where launch mass is the driving constraint. The modularity and reconfigurability provided by the truncated octahedron also allows for significant stability performance improvements. The mass penalty in designing a modular version of a Mars transfer and surface habitat vehicle compared to a “point design,” linear stack concept, was found to be approximately 25%.

For future space exploration, the benefits of modular, reconfigurable spacecraft design are:

- Enhancing mission flexibility: spacecraft could be reconfigured to complete new tasks
- Economic benefits (non-recurring and recurring cost savings)
- Extensible spacecraft design, facilitating an affordable, “Mars back” approach for architecting an affordable and sustainable space exploration system

Both truncated octahedra and cylinders are capable of exhibiting modularity. However, the greater number of interfaces, and hence physical configurations, enabled by truncated octahedra make the shape uniquely suited for architecting spacecraft with complex functional flows and incidental interactions, architecture being the manner in which the functions of a product are mapped to its physical modules. To architect spacecraft with complex functional flows with cylinders requires many more cylinders to embody the functional elements, introducing wasted space, increasing launch costs, and increasing the complexity of the system.

Even for spacecraft whose functional flows are not complex, the greater number of interfaces and configurations permit designers greater flexibility in drawing module boundaries. The greater number of interfaces and configurations also facilitate a greater ease of extensibility associated with bus modularity.

The benefits due to the geometry and modularity of the truncated octahedron are not possible without penalties. A mass penalty is incurred from modularization. Spacecraft complexity is increased due to the increased number of module interconnections. This complexity will likely require sophisticated control systems to be used for autonomous rendezvous and docking of the various spacecraft modules. In addition, initial design cost of a modular space exploration system may be more expensive than an “optimized” system. However, “optimality” over the entire space exploration system lifecycle may favor the modular design approach.

Future work to be performed to further refine the truncated octahedron concept will involve:

- Additional investigation into the extensibility benefits of spacecraft design using the truncated octahedron concept. Spacecraft design extensibility for different vehicles and missions will be studied.
- Application of this concept to the NASA CER project by generating requirements, creating conceptual designs, and performing trade offs to assess the benefits of this concept.
- Design of standardized interfaces between truncated octahedron-shaped modules.
- The application of the rod, ring, and “sphere” structural combinations to overall space exploration mission contexts.
- Manual and autonomous methods for construction and reconfiguration of modules in space.

## Acknowledgments

We thank Wilfried Hofstetter for providing much of the Mars and Moon mission architecture and vehicle conceptual design data used as a design application of this modular spacecraft design concept. Thanks to Justin Wong for an in-depth literature survey and to Thomas Coffee for the investigation into the tiling theory associated with this modular geometry.

## References

<sup>1</sup>Sellers, P. J., “The next manned Earth-to-orbit vehicle (ETOV): What do we need and when do we need it?” White paper available from: PJ Sellers, code CB, NASA/JSC, Houston, Texas, 77058, 2003.

- <sup>2</sup>Likins, P., "Spacecraft Attitude Dynamics and Control – A Personal Perspective on Early Developments," *Journal of Guidance*, Vol. 9, No. 2, March-April 1986, pp. 129–134.
- <sup>3</sup>Frisina, W., "Close-Pack Modules for Manned Space Structures," *Journal of Spacecraft and Rockets*, Vol. 22, No. 5, 1985, pp. 583–584.
- <sup>4</sup>Frisina, W., "Modular Spacecraft," *Journal of Aerospace Engineering*, Vol. 7, No. 4, October 1994, pp. 411–416.
- <sup>5</sup>Parkinson, R. C., "Space Platform - A New Approach to Space Operations," *Proceedings of the 36th Congress of the International Astronautical Federation*, Paris, France, 1985.
- <sup>6</sup>Mikulas, M. M. and Dorsey, J. T., "An Integrated In-Space Construction Facility for the 21st Century," *The 21st Century in Space*, edited by G. V. Butler, Vol. 70, American Astronautical Society, San Diego, CA, 1990, pp. 75–92.
- <sup>7</sup>Whelan, D. A., Adler, E. A., Wilson, S. B., and Roesler, G., "The DARPA Orbital Express Program: Effecting a Revolution in Space-Based Systems," *Small Payloads in Space*, edited by B. J. Horais and R. J. Twiggs, International Society for Optical Engineering, Bellingham, Washington, 2003, pp. 121–128.
- <sup>8</sup>Miller, J., Guerrero, J., Goldstein, D., and Robinson, T., "SpaceFrame: Modular Spacecraft Building Blocks for Plug and Play Spacecraft," *Proceedings of the 16th Annual AIAA/USU Conference on Small Satellites*, Logan, Utah, August 2002.
- <sup>9</sup>Smithies, C., Meerman, M., Wicks, A., Phipps, A., and Sweeting, M., "Microsatellites for Affordable Space Science: Capability and Design Concept," *Proceedings of the 53rd International Astronautical Congress*, Paris, France, October 2002.
- <sup>10</sup>Daniels, M. and Saavedra, B., "The Conestoga Launch Vehicle - A Modular Approach to Meeting User Requirements," *Proceedings of the 15th International Communications Satellite Systems Conference*, San Diego, California, February–March 1994.
- <sup>11</sup>Baily, S., Nelson, R. R., and Stewart, W. B., "Interface Standards for Spacecraft As a Means of Enhancing On-Orbit Servicing," *Proceedings of the 18th Annual Electronics and Aerospace Systems Conference*, Piscataway, New Jersey, 1985, pp. 351–355.
- <sup>12</sup>Harwood, O. P. and Ridenoure, R. W., "A Universal Orbital Docking and Berthing System," *The Case for Mars IV: The International Exploration of Mars, Mission Strategy and Architectures*, edited by T. R. Meyer, Vol. 89, American Astronautical Society, San Diego, California, 1990, pp. 613–630.
- <sup>13</sup>Abbott, R. and Aceves, M., "Self-engaging Connector System for Robotic Outposts and Reconfigurable Spacecraft," *Proceedings of the 2002 IEEE Aerospace Conference*, Vol. 5, Piscataway, New Jersey, 2002, pp. 2165–2170.
- <sup>14</sup>Enright, J., Jilla, C., and Miller, D., "Modularity and Spacecraft Cost," *Journal of Reducing Space Mission Cost*, Vol. 1, No. 2, 1998, pp. 133–158.
- <sup>15</sup>Parkinson, R. C., "Why space is expensive - operational/economic aspects of space transport," *Journal of Aerospace Engineering*, Vol. 205, No. G1, 1991, pp. 45–52.
- <sup>16</sup>Morgenthaler, G. W., "A Cost Trade-Off Model for On-Orbit Assembly Logistics," *Proceedings of the 4th AIAA/SOLE Space Logistics Symposium*, Washington D.C., 1991, pp. 503–524.
- <sup>17</sup>Ulrich, K. and Tung, K., "Fundamentals of Product Modularity," *ASME Issues in Design Manufacture/Integration*, Vol. 39, Atlanta, Georgia, December 1991, pp. 73–79.
- <sup>18</sup>Mikkola, J. H. and Gassmann, O., "Managing Modularity of Product Architectures: Toward an Integrated Theory," *IEEE Transactions on Engineering Management*, Vol. 50, No. 2, May 2003, pp. 204–218.
- <sup>19</sup>Vogel, S., *Cats' Paws and Catapults*, W. W. Norton and Company, London, England, 1998.
- <sup>20</sup>Hartke, C. A., "The Illinois Bees and Apiaries Program Photo Gallery," [www.agr.state.il.us/programs/bees/pages/bee-with\\_honeycomb.htm](http://www.agr.state.il.us/programs/bees/pages/bee-with_honeycomb.htm).
- <sup>21</sup>Dress, A. W. M., Huson, D. H., and Molnár, E., "The Classification of Face-Transitive Periodic Three-Dimensional Tilings," *Acta Crystallographica*, Vol. A49, 1993, pp. 806–817.
- <sup>22</sup>Bush, P. G. W., "A Renewed Spirit of Discovery: The President's Vision for U.S. Space Exploration," January 2004.
- <sup>23</sup>Hofstetter, W., *Extensible Modular Landing Systems for Human Moon and Mars Exploration*, Master's thesis, Technische Universität München, 2004.
- <sup>24</sup>Project, . A. S., "NASA Concept Evaluation and Refinement Study," Massachusetts Institute of Technology, fall 2004.
- <sup>25</sup>"The Reference Mission of the NASA Mars Exploration Study Team," NASA Special Publication 6017, July 1997.
- <sup>26</sup>Systems, B. I. D., "Delta IV Heavy Growth Options for Space Exploration," [www.boeing.com/defense-space/space/bls/d4heavy/docs/delta\\_growth\\_options.pdf](http://www.boeing.com/defense-space/space/bls/d4heavy/docs/delta_growth_options.pdf).
- <sup>27</sup>Isakowitz, S. J., Hopkins, J. B., and J. P. Hopkins, J., *International Reference Guide to Space Launch Systems*, American Institute of Aeronautics and Astronautics, Reston, Virginia, 2004.
- <sup>28</sup>Woolford, B. and Bond, R. L., "Human Factors of Crewed Spaceflight," *Human Spaceflight Mission Analysis and Design*, edited by W. J. Larson and L. K. Pranke, McGraw Hill, New York, New York, 1999, pp. 149–150.
- <sup>29</sup>Petro, A., "Transfer, Entry, Landing, and Ascent Vehicles," *Human Spaceflight Mission Analysis and Design*, edited by W. J. Larson and L. K. Pranke, McGraw Hill, New York, New York, 1999, pp. 403–404.
- <sup>30</sup>Messerschmid, E. and Bertrand, R., *Space Stations: Systems and Utilization*, Springer, Berlin, Germany, 2004.
- <sup>31</sup>Fortescue, P. and Stark, J., *Spacecraft Systems Engineering*, John Wiley and Sons, Chichester, West Sussex, England, 2nd ed., 1995, p. 161.
- <sup>32</sup>Farquhar, R. W., Dunham, D. W., Guo, Y., and McAdams, J. V., "Utilization of Libration Points for Human Exploration in the Sun-Earth-Moon System and Beyond," *Proceedings of the 54th International Astronautical Congress of the International Astronautical Federation*, Bremen, Germany, September-October 2003.
- <sup>33</sup>Aeronautics, N. and Administration, S., "Apollo 11 Press Kit," NASA Public Affairs Office, 1969.
- <sup>34</sup>Kaplan, M. H., *Modern Spacecraft Dynamics and Control*, John Wiley and Sons, New York, New York, 1976.